Journal of Medicinal Chemistry

Article

pubs.acs.org/jmc

EC144 Is a Potent Inhibitor of the Heat Shock Protein 90

Jiandong Shi,[†] Ryan Van de Water,[†] Kevin Hong,[†] Ryan B. Lamer,[†] Kenneth W. Weichert,[†] Cristina M. Sandoval,[†] Srinivas R. Kasibhatla,[†] Marcus F. Boehm,[†] Jianhua Chao,[†] Karen Lundgren,[†] Noelito Timple,[†] Rachel Lough,[†] Gerardo Ibanez,[†] Christina Boykin,[†] Francis J. Burrows,[†] Marilyn R. Kehry,[†] Theodore J. Yun,[†] Erin K. Harning,[†] Christine Ambrose,[‡] Jeffrey Thompson,[‡] Sarah A. Bixler,[‡] Anthone Dunah,[‡] Pamela Snodgrass-Belt,[‡] Joseph Arndt,[‡] Istvan J. Enyedy,[‡] Ping Li,[‡] Victor S. Hong,[‡] Andres McKenzie,[‡] and Marco A. Biamonte*[,†]

[†]Biogen Idec, 5200 Research Place, San Diego, California 92122, United States

[‡]Biogen Idec, 14 Cambridge Center, Cambridge, Massachusetts 02142, United States

Supporting Information

ABSTRACT: Alkyne **40**, 5-(2-amino-4-chloro-7-((4-methoxy-3,5-dimethylpyridin-2-yl)methyl)-7*H*-pyrrolo[2,3-*d*]pyrimidin-5-yl)-2-methylpent-4-yn-2-ol (EC144), is a second generation inhibitor of heat shock protein 90 (Hsp90) and is substantially more potent in vitro and in vivo than the first generation inhibitor **14** (BIIB021) that completed phase II clinical trials. Alkyne **40** is more potent than **14** in an Hsp90α binding assay (IC_{50} = 1.1 vs 5.1 nM) as well as in its ability to degrade Her-2 in MCF-7 cells (EC_{50} = 14 vs 38 nM). In a mouse model of gastric tumors (N87), **40** stops tumor growth at 5 mg/kg and causes partial tumor regressions at 10 mg/kg (po, qd×5). Under the same conditions, **14** stops tumor growth only at 120 mg/kg, and does not induce partial regressions. Thus, alkyne **40** is approximately 20-fold more efficacious than **14** in mice.

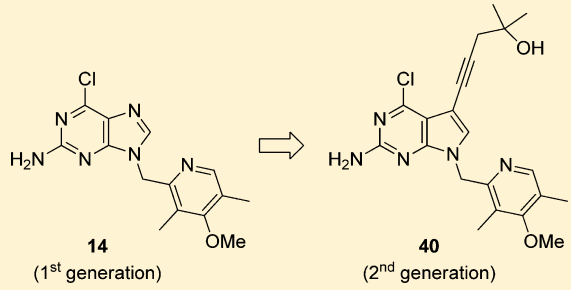

1. INTRODUCTION

The rationale for selecting heat shock protein 90 (Hsp90) as a cancer target has been extensively reviewed.[1] In essence, Hsp90 regulates the folding of nascent and mature proteins, collectively dubbed "client proteins". Among the over 200 reported Hsp90 client proteins,[2] one finds a large proportion of proteins implicated in cell-growth, including well-known oncogenes (Raf-1, Akt, cdk4, Src, Flt-3, hTert, c-Met, etc.) and five proteins targeted by approved cancer drugs: Her-2/neu (trastuzumab), Bcr-Abl (imatinib), the estrogen receptor (tamoxifen), the androgen receptor (bicalutamide), and VEGF, the vascular endothelial growth factor receptor (sunitinib). Inhibition of Hsp90 causes client proteins to adopt aberrant conformations, and these abnormally folded proteins are eliminated via ubiquitination and proteasome degradation. The net result is that Hsp90 inhibitors induce the concomitant degradation of a number of oncogenes and therefore intervene simultaneously on different pathways of cancer progression.

In 1998−1999, the first clinical trials with an Hsp90 inhibitor were initiated on the natural product derivative 17-allylamino-17-desmethoxygeldanamycin **1** (17-AAG, tanespimycin, Cancer Research UK, NCI, Scheme 1). 17-AAG was administered intravenously and progressed to phase III studies (Kosan-Bristol Myers Squibb).[3] Although 17-AAG was poorly water-soluble and difficult to formulate, its hydroquinone version **2** (IPI-504, retaspimycin, Infinity) could be converted to a water-soluble hydrochloride salt which also advanced to phase III studies.[4] The derivative 17-desmethoxy-17-*N*,*N*-dimethylaminoethylaminogeldanamycin **3** (17-DMAG, alvespimycin, NCI, Kosan-Bristol Myers Squibb) was also designed to improve the solubility but proved to be more toxic in preclinical species.[5] The major metabolite of 17-AAG, 17-amino-17-desmethoxygeldanamycin **4** (17-AG, IPI-493, Infinity), displayed greatly improved oral bioavailability and was advanced as an oral formulation, thus obviating the need for solubility imposed by the intravenous route of administration.[6] In parallel, 12 fully synthetic small molecules were developed (Scheme 1), as either intravenous or oral compounds. The intravenous drugs are **5** (NVP-AUY922, Novartis, phase II),[7] **6** (AT-13387, Astex, phase II),[8] **7** (ganetispib, STA-9090, Synta, phase II),[9] **8** (KW-2478, Kyowa Hakko Kirin, phase I/II),[10] **9** (XL-888, Exelixis, phase I),[1a] **10** (PU-H71, Memorial Sloan-Kettering Cancer Center, phase I),[11] and BIIB028 (Biogen Idec, phase I, structure not public). The oral drugs are **11** (DEBIO-0932/CUDC305, Debiopharm, phase I),[12] **12** (MPC-3100, Myrexis, phase I),[13] **13a** (PF-4929113/SNX-5422, Pfizer, phase I), which is a glycine prodrug of **13b**,[14] **14** (BIIB021, Biogen Idec, phase II),[15] and **15** (NVP-HSP990, Novartis, phase I).[16]

As of this writing, the major challenge in the Hsp90 arena is to identify which human cancers best respond to an Hsp90

Received: June 8, 2012
Published: August 31, 2012

 © 2012 American Chemical Society

Scheme 1. Hsp90 Inhibitors in Clinical Trials

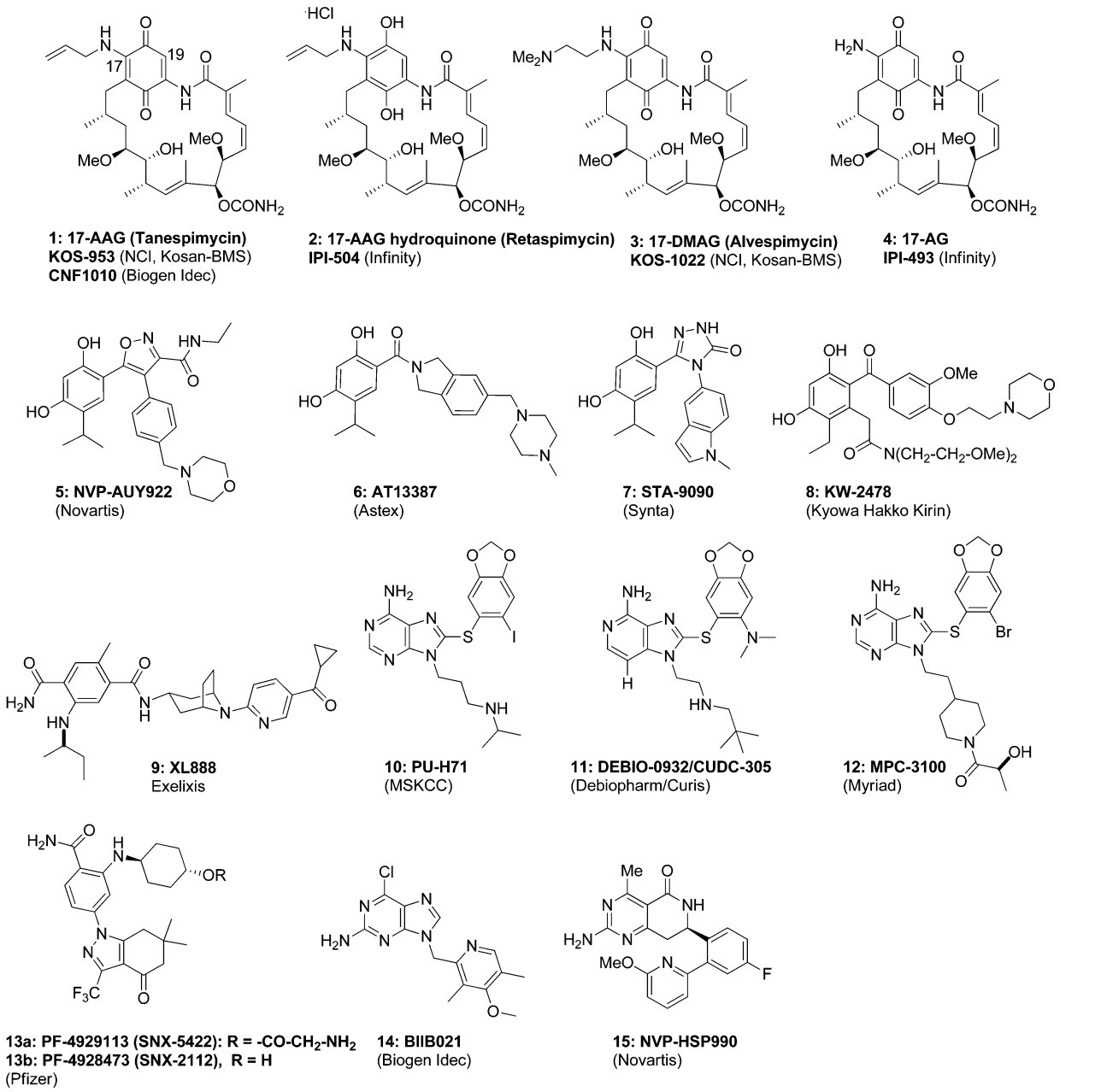

inhibitor and with which drug combination. Breast cancer is the most studied indication for Hsp90 inhibitors. The rationale is simple: some breast cancers are Her-2 driven, and Her-2 is degraded particularly rapidly upon exposure to Hsp90 inhibitors. Furthermore, Her-2 is the molecular target of the breast cancer drug trastuzumab. In a notable phase II trial, patients with Her-2 positive metastatic breast cancer that were progressing on trastuzumab responded to the combination of 17-AAG and trastuzumab, with a 22% overall response rate.[17] This was the first phase II study in which 17-AAG definitely showed responses in solid tumors, as defined by the response evaluation criteria in solid tumors (RECIST). In addition to breast cancer, non-small-cell lung cancer (NSCLC) and multiple myeloma (MM) also appear to be of high interest. In phase II studies in NSCLC patients, retaspimycin and resorcinol 7 controlled the disease in a subset of patients harboring a mutated/rearranged anaplastic lymphoma kinase (ALK).[18,19] This is consistent with the fact that ALK is the only Hsp90 client showing equivalent or greater sensitivity than Her-2 to Hsp90 inhibitors.[1a] ALK + NSCLC can be treated with the approved ALK inhibitor crizotinib, but resistance appears within 1 year. In vitro, the combination of crizotinib with an Hsp90 inhibitor overcomes the crizotinib resistance.[20] In a phase I/II study in a MM population, the combination of 17-AAG and bortezomib gave an objective response rate of 27% and was also active in patients that were refractory to bortezomib.[21] Interestingly, at the preclinical level there is evidence that even low doses of Hsp90 inhibitors can be strongly synergistic with radiation therapy in head and neck squamous cell carcinoma.[22] All Hsp90 inhibitors cause fatigue

dx.doi.org/10.1021/jm300810x | J. Med. Chem. 2012, 55, 7786−7795

Scheme 2[a]

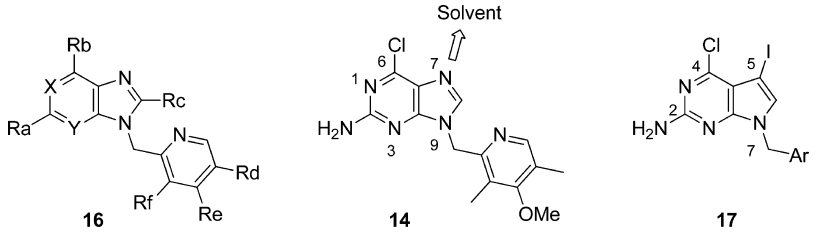

[a]Modifications of **16** in positions Ra–Rf led to a decrease in potency, suggesting that the solvent exposed area of the molecule was pointing in the same direction as the N7 lone pair of purine **14**.

and diarrhea as side effects, and some but not all also produce ocular toxicities, which led to the discontinuation of benzamide **13a**.[23,24]

In 2005, we selected purine **14** as clinical candidate because it was the first orally bioavailable Hsp90 inhibitor that consistently demonstrated efficacy in mouse tumor models.[15] The fact that it could be synthesized in a single step was an additional advantage.[15] There was a limitation, however, in that high doses (60–120 mg kg^{-1} day^{-1}) were required for efficacy in mouse. In human, even though the doses of **14** may be lower, treating patients still requires 100 mg twice daily or 450 mg thrice weekly, as proposed in a phase II study conducted in combination with exemestane (Aromasin, 25 mg daily) for hormone receptor positive metastatic breast cancer (HR + mBC). While running clinical trials with **14**, we sought a second generation oral Hsp90 inhibitor that would be more efficacious than **14** to allow for lower daily or weekly dosing. We now report the chemistry that led to a series of deazapurine analogues, some of which showed efficacy in mouse tumor models at 5 mg/kg and represent an improvement of over 1 logarithm over the first generation inhibitors.

2. ASSAYS

HSP90 exists as two isoforms: HSP90α is an inducible form overexpressed in cancer cells, while HSP90β is the constitutive form. Both HSP90α and HSP90β are found in the cytoplasm. There are also two paralogues: Grp94, localized in the endoplasmic reticulum lumen, and TRAP1, confined to mitochondria. The binding assays were performed on HSP90α as described previously.[25]

The effect of HSP90 inhibitors on breast cancer MCF-7 cells was evaluated by measuring the degradation of the HSP90 client Her-2. Her-2, being a cell-surface receptor, can be conveniently monitored with extracellular-directed fluorescent antibodies and flow cytometry.[25]

For in vivo work, and unless otherwise noted, **40** was suspended in an aqueous solution containing 0.5 wt % carboxymethylcellulose (CMC) and 0.1 wt % Tween 80. The suspension was sonicated for 30 min at room temperature and homogenized for 30 s using a homogenizer set at 4000 rpm. Alternatively, **40** was dissolved in 0.1 N HCl, and the two formulations gave comparable results. Pharmacokinetic parameters were determined by analyzing extracted plasma and tissue samples by LC/MS/MS and by using noncompartmental methods with WinNonlin, version 5 (Pharsight).

3. DESIGN AND SYNTHESIS OF THE PYRROLO[2,3-*D*]PYRIMIDINE SCAFFOLD

The optimization of **14** was challenging, as all attempts to modify the substituents Ra–Rf (Scheme 2) typically led to a drastic decrease in potency. Similarly, replacement of X or Y by a carbon atom also led to a loss in potency. We therefore hypothesized that each of these positions was in close contact with the protein. Yet it seemed logical to expect that at least one part of the molecule would face the solvent and that modifications of the solvent-exposed area of the molecule would be the most tolerable. We felt that the solvent-exposed area may be used to our advantage to improve the drug properties and to possibly gain potency by making new interactions at the rim of the binding pocket. Since the substituents Ra–Rf, as well as the atoms X and Y, were clearly failing at reaching the solvent-exposed area, we deduced that the solvent-exposed area must have been pointing in another direction. By elimination, we surmised that the solvent was facing the direction of the N7 lone pair, and this initial hypothesis was later validated by an X-ray structure (Figure 1).

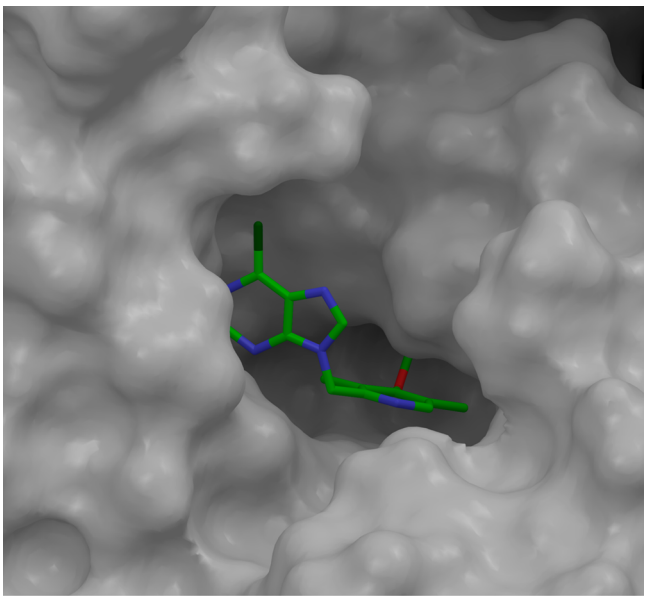

Figure 1. The X-ray structure of **14** in complex with Hsp90 shows that N7 faces a solvent exposed area (PDB code: 3QDD).

In order to substitute the molecule along the desired vector, it was necessary to replace N7 with a carbon atom. To this effect, we prepared pyrrolo[2,3-*d*]pyrimidines (=deazapurines) based on scaffold **17** (Scheme 2) where the iodo group would enable a range of cross-couplings. The synthesis started with 2,6-diaminopyrimidin-4-ol **18** (Scheme 3). The next four steps relied on existing procedures[26–30] that were modified to increase the yield of **23** and to obviate the need for chromatographic purifications. Thus, treatment of **18** with

dx.doi.org/10.1021/jm300810x | *J. Med. Chem.* 2012, 55, 7786–7795

Scheme 3. Preferred Synthesis of Pyrrolo[2,3-*d*]pyrimidine 27

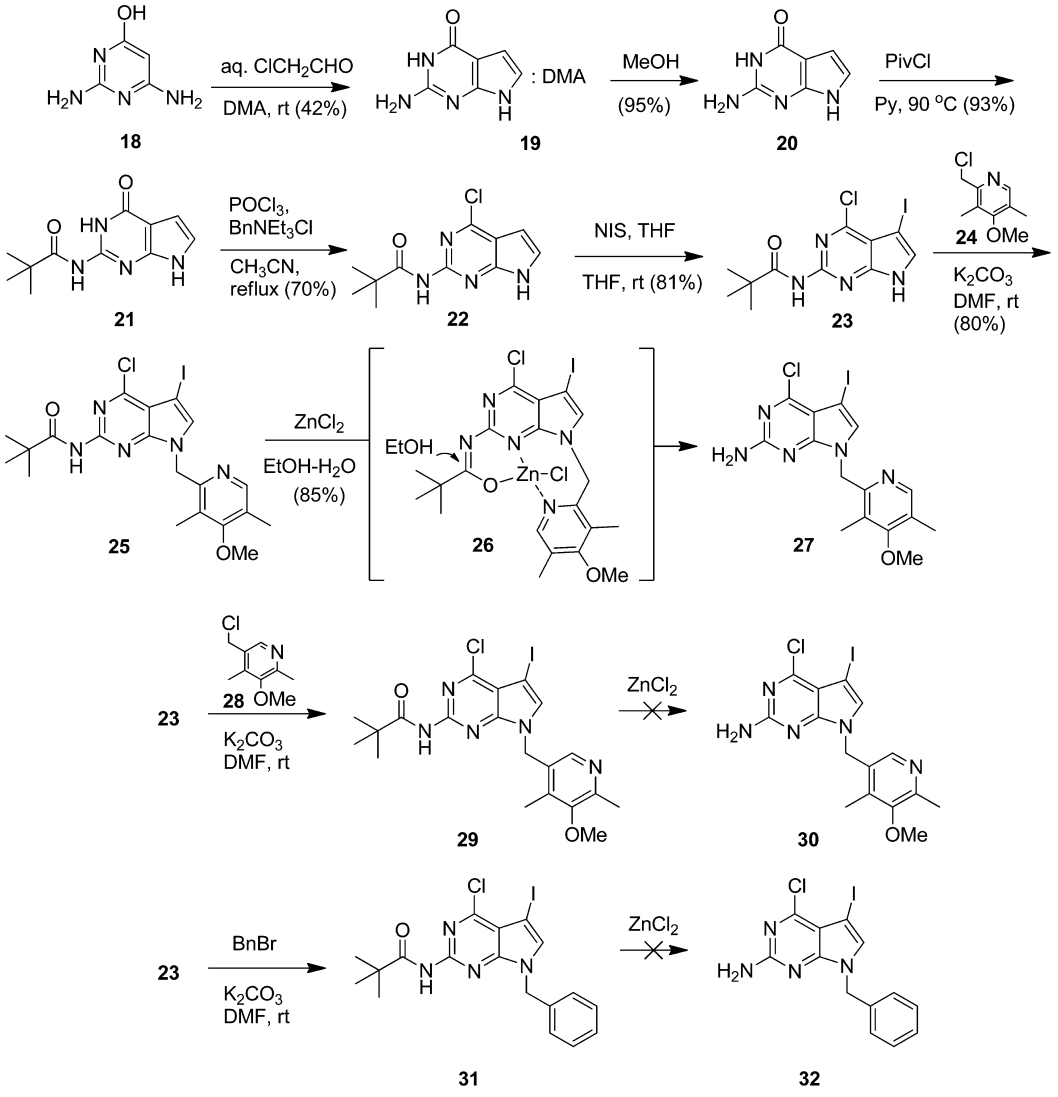

Scheme 4. Alternative Synthesis to Pyrrolo[2,3-*d*]pyrimidine 27 and Synthesis of 35

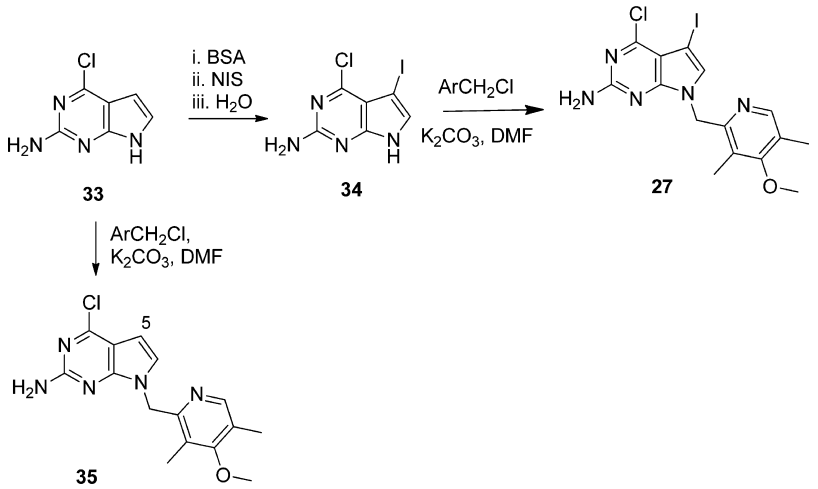

aqueous chloroacetaldehyde provided the pyrrolo[2,3-*d*]-pyrimidine **19** (42%). By performing this cyclization in the presence of *N*,*N*-dimethylacetamide (DMA) as opposed to DMF,[26] the desired product precipitated out as a 1:1 DMA complex, which facilitated its production on kilogram scale. The DMA was then easily removed by recrystallization from MeOH (95%). Protection of the amino group with PivCl gave amide **21** (93%).[27] Deoxychlorination[28] was best achieved with a

dx.doi.org/10.1021/jm300810x | *J. Med. Chem.* 2012, 55, 7786−7795

Scheme 5[a]

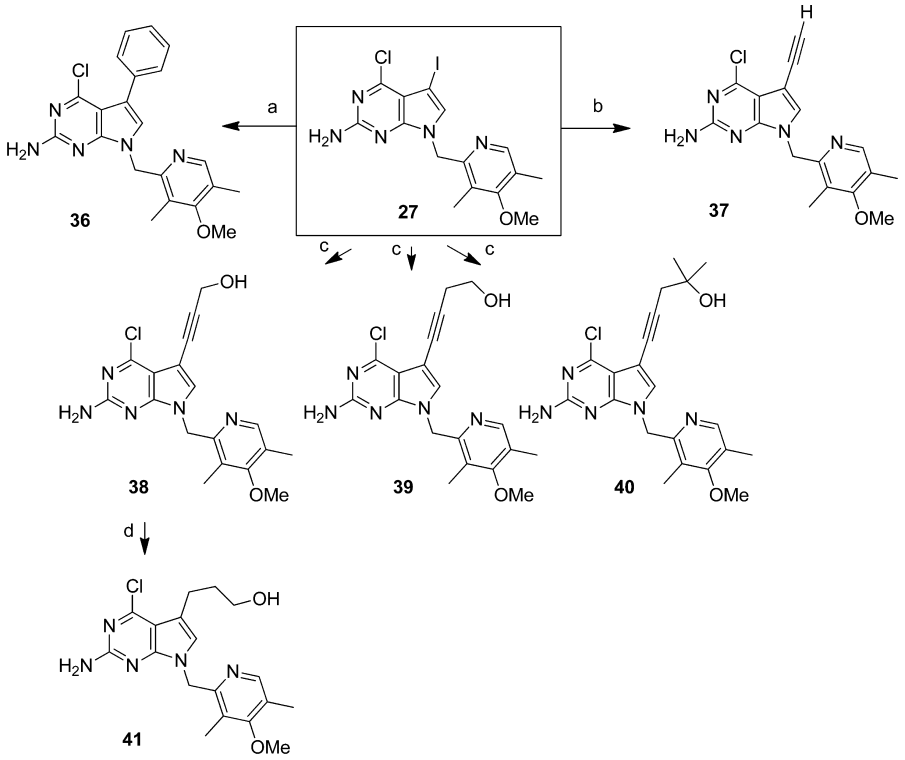

[a]Conditions: (a) $PhB(OH)_2$, $Pd(PPh_3)_4$, DMF, 2 M K_2CO_3, 80 °C (20%); (b) $HC{\equiv}C{-}SiMe_3$, Et_3N, CuI, $Pd(PPh_3)_4$, DMF, 50 °C (25−50%), then TBAF, THF, rt (25%); (c) alkyne, Et_3N, CuI, $Pd(PPh_3)_4$, DMF, 50 °C (25−50%), or alkyne, Et_3N, CuI, 10% Pd/C, PPh_3, H_2O, DMA or DMSO, 75 °C (40−75%); (d) Raney Ni, H_2 (4.5 atm), MeOH, rt (32%).

$POCl_3$/$BnNEt_3Cl$ system to give **22** (70%), and a subsequent iodination with *N*-iodosuccinimide (NIS)[29,30] yielded **23** regioselectively (81%). It is noteworthy that the pivaloyl group was necessary for both the deoxychlorination and the iodination to proceed smoothly. Attempts at replacing the pivaloyl group with an acetyl or octanoyl group resulted in a complex mixture of products upon sequential treatment with $POCl_3$ and NIS. However, cleaving the pivaloyl group proved to be a difficult operation. After extensive experimentation, we found that the pivaloyl group could be efficiently removed if **23** was first alkylated with the commercially available chloromethylpyridine **24** (80%) and then treated with $ZnCl_2$ in refluxing EtOH, thus yielding the key intermediate **27** (85%). Interestingly, this deprotection procedure was successful only if **23** was alkylated with **24** prior to treatment with $ZnCl_2$. Alkylation of **23** with the isomeric chloromethylpyridine **28** gave substrate **29**, which failed to undergo the $ZnCl_2$-mediated deprotection. Similarly, alkylation of **23** with benzyl bromide gave substrate **31** that was equally unreactive toward $ZnCl_2$. To rationalize these results, we suggest that the pyridine nitrogen of **25** is actively involved in the transition state, possibly by offering an additional coordination site for the Zn atom as shown in the putative intermediate **26**. The entire sequence **18** → **27** could be performed without any chromatographic purification on kilogram scale.

In an alternative route (Scheme 4), pyrrolo[2,3-*d*]pyrimidine **33** was temporarily silylated with *N*,*O*-bis(trimethylsilyl)-acetamide (BSA), reacted with NIS, and desilylated with water to give iodide **34** in a single pot.[31] Iodide **34** was poorly soluble in organic solvents, which precluded further purification. Iodide **34** could nonetheless be alkylated to give **27**. For SAR purposes, compound **33** was also directly alkylated to give pyrrolopyrimdine **35**, devoid of any substituent at C5.

4. OPTIMIZATION OF POTENCY

Having devised two efficient syntheses of iodide **27**, we submitted it to Pd cross-couplings (Scheme 5). A Suzuki coupling with $PhB(OH)_2$ gave the 5-phenyl adduct **36**, while Sonogashira couplings with TMS acetylene, propargylic alcohol, homopropargylic alcohol, or with 2-methylpent-4-yn-2-ol[32] gave derivatives **37**−**40**. Hydrogenation of propargylic alcohol **38** with Raney nickel gave propanol **41**. The reactions leading to **37**−**41** were not optimized. All compounds were prepared in greater than 95% purity as determined by analytical HPLC at 254 nm.

In a biochemical assay, compounds **35**−**41** all bound to Hsp90α with IC_{50} < 10 nM (Table 1). Next, their ability to induce the degradation of Her-2 in MCF-7 breast cancer cells was examined (Table 1). The first-generation clinical candidate **14** degraded Her-2 with EC_{50} = 38 nM. In the same assay, the unsubstituted pyrrolo[2,3-*d*]pyrimidine **35** (EC_{50} = 100 nM) was almost as active as **14**. More importantly, substituents at the C5 position were tolerated. Compared to **35**, a phenyl substituent (**36**, 250 nM) only led to a 2.5-fold decrease in potency, while a terminal alkyne group (**37**, 26 nM) improved the potency 4-fold. The propargyl alcohol **38** (15 nM) and the homopropargylic alcohols **39** (9 nM) and **40** (EC144, 14 nM) were the most potent compounds and were approximately 3-fold more potent in vitro than the first-generation clinical candidate **14**. Reduction of the propargylic alcohol **38** to the propanol **41** (32 nM) was tolerated.

dx.doi.org/10.1021/jm300810x | J. Med. Chem. 2012, 55, 7786−7795

Table 1. Hsp90 Inhibitors: Binding to Hsp90α and Effect on the Degradation of Her-2 in MCF-7 Cells

inhibitor	R	binding Hsp90α IC_{50} [nM]	Her-2 EC_{50} [nM]
17-AAG			12 ± 5
5 (resorcinol)		<0.4	7 ± 1
13b (benzamide)		3	19 ± 3
14 (purine)		5.1 ± 2.0	38 ± 13
35	H		98 ± 3
36	Ph	6.0 ± 2.8	250 ± 14
37	C≡CH	1.0 ± 0.6	26 (n = 1)
38	C≡C−CH_2OH	0.7 (n = 1)	15 ± 7
39	C≡C−$(CH_2)_2$OH	2.0 ± 1.3	9 ± 3
40	C≡C−CH_2−CMe_2OH	1.1 ± 0.5	14 ± 5
41	CH_2− CH_2−CH_2OH	3.9 (n = 1)	32 ± 5

Thus, compounds **38**−**40** were the most potent ones in vitro. This article focuses on compound **40**, since it later proved to have the best combination of pharmacokinetic properties and efficacy in murine cancer models.[33]

A crystal structure of **40** in complex with Hsp90 revealed a favorable hydrophobic interaction between the C≡C fragment of the inhibitor and the adjacent side chains of Met-98 and Leu-107 (Figure 2).[34] There were no other obvious additional interactions. The distance between the OH group and the Lys-58 amino group was too large (4.3 Å) for a hydrogen bond, although the solution structure may differ from the crystal structure, possibly granting the side chain of Lys-58 enough flexibility to form a hydrogen bond in solution.

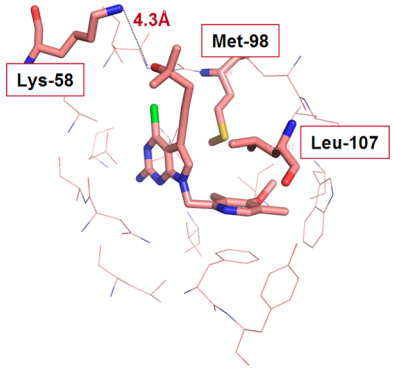

Figure 2. X-ray structure of alcohol **40** in complex with Hsp90α (PDB code: 3NMQ).

5. SELECTIVITY

The tertiary alcohol **40** binds to Hsp90α with K_i = 0.2 nM and is selective against the Hsp90 paralogues TRAP1 (K_i = 255 nM) and Grp94 (K_i = 61 nM).[34] Alcohol **40** has no inhibitory activity (IC_{50} > 10 μM) against a panel of 285 human kinases.[34] When incubated with N87 (gastric) or BT474 (breast) tumor cell lines, **40** displays the characteristic signature of Hsp90 inhibitors: degradation of the client proteins (Her-2, EGFR, IGFR, ERK, Akt, Rb, cyclin D, cdk6), up-regulation of Hsp70, and no effect on p85 PI3K, which is not a Hsp90 client (data not shown for cell cultures, see section 7 for in vivo data).

6. IN VITRO ADMET AND IN VIVO PK

Alcohol **40** satisfies the "rule of five" by virtue of its two hydrogen-bond donors, four hydrogen bond acceptors, a molecular weight of 414, and a cLogP of 2.8. Alcohol **40** is highly permeable in CACO-2 cells (34.7×10^{-6} cm/s, Table 2) and is not actively effluxed (efflux ratio (B → A)/(A → B) = 1.1). The lack of efflux is similar to what was observed with the first-generation purine **14** (efflux ratio = 1.5) and contrasts with the behavior of resorcinol **5** (efflux ratio = 15) and benzamide **13b** (efflux ratio = 35). Alcohol **40** is 94−97% protein bound depending on the species and in this respect is similar to resorcinol **5** (94−96%) and benzamide **13b** (90−94%). Alcohol **40** is metabolized by microsomes at medium−high rates; the intrinsic hepatic clearance is 119 mL min^{-1} kg^{-1} in human microsomes, which is higher than for resorcinol **5** (39 mL min^{-1} kg^{-1}) and benzamide **13b** (54 mL min^{-1} kg^{-1}).

In mice, the maximum tolerated dose (MTD) of alkyne **40** for a *single* oral administration is 30 mg/kg. Table 3 reports the mouse pharmacokinetic data for a single oral dose of **40**, compared with the data for other known Hsp90 inhibitors. At 25 mg/kg, the plasma exposure of **40** is 4419 ng·h/mL. In contrast, the first-generation inhibitor **14** required a dose of 100 mg/kg to give a comparable exposure. This may be more evident by looking at the AUC/dose ratio which, if expressed in (ng·h/mL)/(mg/kg), gives 48 for purine **14** and 177 for alcohol **40**. Alcohol **40** is cleared with a $T_{1/2}$ of 1.5 h, which is somewhat longer than for purine **14** (0.8 h) but shorter than for benzamide **13** (2.9 h) and resorcinol **5** (6.6 h).

A tissue-distribution study (Table 4) indicates that **40** distributes well to the brain, spleen, and lymph nodes. Alcohol **40** crosses the blood-brain barrier (brain/plasma = 2.2), which is consistent with the fact that it is not an efflux substrate.

7. APPLICATIONS TO ONCOLOGY

Hsp90 inhibitors have been reported to be retained in tumors. Alkyne **40** was administered in a single dose of 6 or 12 mg/kg to mice bearing xenografts of N87 gastric tumors (Figure 3). Tumors were collected 1, 6, and 24 h after dosing and analyzed. At the 6 and 24 h time-points, the concentration of alkyne **40** was highest in the tumors and decreased in the order tumors > spleen > brain > serum, indicating that tumors retain alkyne **40** better than other tissues as time progresses (Figure 3).

Table 2. In Vitro ADME Parameters of Selected Hsp90 Inhibitors[a]

	CACO-2 permeability [$\times 10^{-6}$ cm/s]		protein binding, fraction unbound [%]			microsomal intrinsic hepatic clearance [mL min^{-1} kg^{-1}]		
	P_{app} (A → B)	ratio (B → A)/(A → B)	mouse	rat	human	mouse	rat	human
5 (resorcinol)	1.9	15	4.3	6.4	5.1	443	219	39
13b (benzamide)	1.1	35	6.0	9.6	6.8	301	54	54
14 (purine)	20	1.5			11.4			
40	34.7	1.1	3.4	5.8	3.3	727	276	119

[a]Errors on the protein binding are in the ±0.2−0.9 range.

dx.doi.org/10.1021/jm300810x | J. Med. Chem. 2012, 55, 7786−7795

Table 3. Pharmacokinetic Data for Selected Hsp90 Inhibitors in CD-1 Mouse after a Single Oral or Intravenous Administration[a]

compd	ROA	dose [mg/kg]	$C_{max,Co}$ [ng/mL]	T_{max} [h]	AUC [ng·h/mL]	AUC/dose [(ng·h/mL)/(mg/kg)]	$T_{1/2}$ [h]
5 (resorcinol)	iv	5	2180		2409	481	6.6
13 (benzamide)	po	25	1724	1.0	8517	341	2.9
14 (purine)	po	100	10000	0.083	4800	48	0.8
40	po	25	1556	0.5	4419	177	1.5

[a]Benzamide **13** was administered as its prodrug **13a**, and the PK parameters refer to its active metabolite **13b**.

Table 4. Pharmacokinetic Data for 40 in DBA1 Mouse after a Single po Administration of 5 mg/kg

tissue	C_{max} [ng/mL]	T_{max} [h]	AUC_{inf} [ng·h/mL]	$T_{1/2}$ [h]	tissue/plasma (AUC ratio)
plasma	835	0.083	2118	1.2	
brain	1446	0.5	4713	2.1	2.2
lymph nodes	2144	1.0	5186	1.6	2.4
spleen	1887		8159	2.0	3.9

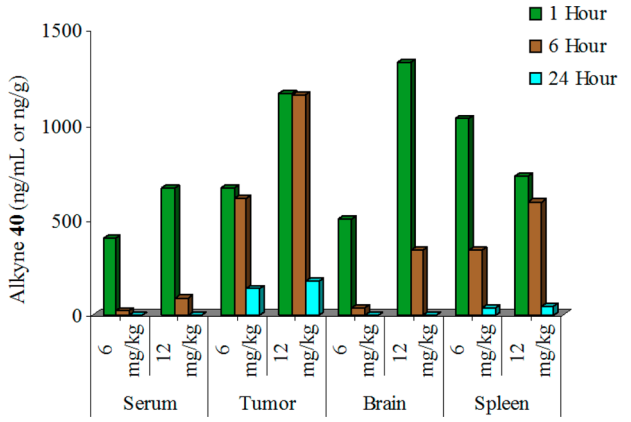

Figure 3. Retention of alkyne **40** in tumors. Mice bearing N87 xenografts were administered a single dose of 6 or 12 mg/kg alkyne **40**. The concentration of alkyne **40** was measured in the serum, tumors, brain, and spleen at 1, 6, and 24 h postdose.

The pharmacodynamic profile of alkyne **40** was evaluated by treating mice bearing breast-cancer BT474 tumors with a single oral dose of 4 or 8 mg/kg (Figure 4). Alkyne **40** induces the typical signature of Hsp90 inhibitors: degradation of the Hsp90 clients Her-2, pHer-2, pAKT, pRAf, pERK, cdk6, pRb, up-regulation of Hsp70 and Hsp27, and no effect on PI3K, which is not an Hsp90 client. Of note, the pharmacodynamic effect of **40** is long lasting. Since cells require 24−48 h to resynthesize the client proteins, even a relatively brief exposure to **40** (plasma $T_{1/2}$ = 1.2 h) results in a protracted pharmacodynamic response that lasts >24 h. A similar effect was reported for purine **14** and has been colloquially called a "hit-and-run effect".[1c] In addition, as mentioned above, **40** is retained in tumors for longer than in the plasma.

In a N87 gastric tumor xenograft model, **40** caused tumor stasis when dosed 5 days per week at 5 mg/kg and induced partial tumor regressions at 10 mg/kg (Figure 5). This is a significant increase in potency when compared to **14**, which was not quite as effective, even at 120 mg/kg, and which did not cause partial regressions. The increase in potency of **40** was accompanied by a commensurate increase in toxicity, and the MTD of **40** on a 5 days per week schedule was 10 mg kg^{-1} day^{-1}. Above the MTD, weight loss and diarrhea were

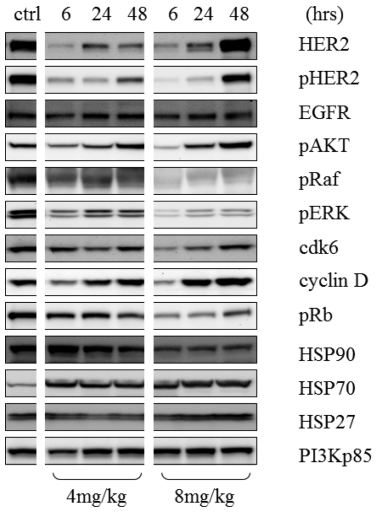

Figure 4. Pharmacodynamic effect of alkyne **40**. Mice bearing BT474 xenografts were treated with a single oral dose of 4 or 8 mg/kg alkyne **40**. Tumors were collected for Western blot analysis at 6, 24, and 48 h postdose.

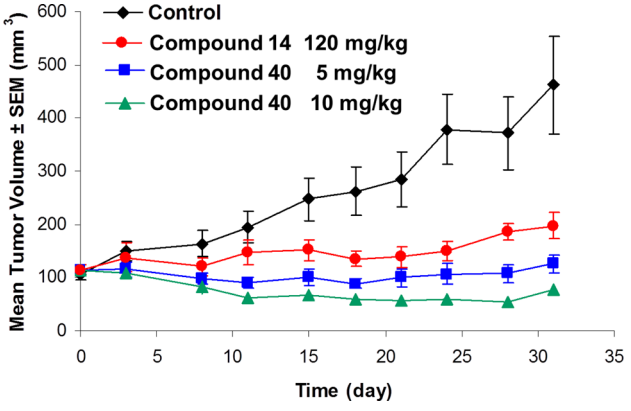

Figure 5. Inhibition of tumor growth in the N87 gastric tumor model. Athymic mice bearing established N87 gastric tumor xenografts were treated with vehicle control, purine **14**, or alcohol **40** orally qd×5 for 4 weeks.[35] Tumors were measured using Vernier calipers on the indicated days, and tumor volumes are reported as mean volume ± SEM tumor for groups of eight mice.

observed, as is typical of all Hsp90 inhibitors. The fact that the toxicity increases proportionally with the efficacy was seen with every Hsp90 inhibitor we tested, irrespective of its chemical class, suggesting that the toxicity is consistently mediated by Hsp90 (on-target).

Alcohol **40** was also tested in a PGP overexpressing adrenocortical carcinoma model (Figure 6) and was active at 8 mg/kg. Purine **14** was less potent but still inhibited tumor growth at 120 mg/kg. In contrast, 17-AAG, which is a known

dx.doi.org/10.1021/jm300810x | J. Med. Chem. 2012, 55, 7786−7795

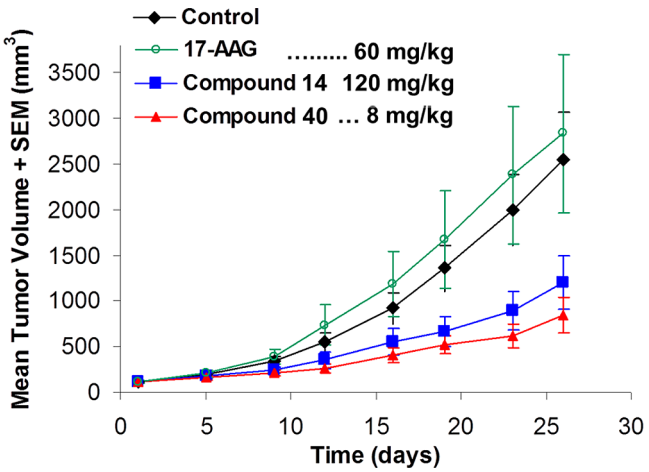

Figure 6. Inhibition of tumor growth in the PGP overexpressing NCI295 adrenal carcinoma. Athymic mice bearing established NCI295 carcinoma were treated with vehicle control, purine **14** (120 mg/kg, po), alcohol **40** (8 mg/kg, po), or 17-AAG (60 mg/kg, ip), qd×5 for 4 weeks. Tumors were measured using Vernier calipers on the indicated days, and tumor volumes are reported as the mean volume ± SEM tumor for groups of seven mice.

PGP substrate,[36] did not slow tumor progression at its MTD (60 mg/kg, iv). Thus, this PGP-overexpressing tumor responded much better to **40** than to the PGP substrate 17-AAG.

8. APPLICATIONS TO IMMUNOLOGY

The applications of **40** to inflammatory and autoimmune conditions are reported in a separate publication, where alcohol **40** is shown to block inflammatory and immune processes in vitro and in vivo.[34] Alcohol **40** inhibited TNF-α release by LPS administration in an LPS shock model. Furthermore, **40** also suppressed disease development in T cell driven rodent collagen-induced arthritis models.[34]

9. APPLICATIONS TO NEUROLOGY

Inhibition of Hsp90 has been shown to lead to the degradation of aberrant forms of p-tau,[37] which aggregate to form neurofibrillary tangles. Such tangles are a hallmark of Alzheimer's disease (AD).[38−41] Since **40** distributes well across the BBB (brain/plasma ratio of 2.2), we examined if **40** could reach pharmacologically relevant concentrations in the brain by monitoring the up-regulation of brain Hsp70. Up-regulation of Hsp70 is the pharmacodynamic response expected of Hsp90 inhibitors. Groups of four B6D2F1 female mice were administered a single oral dose of vehicle alone or compound **40** at several dose levels (Figure 7). The animals were humanely sacrificed 24 h later, and Hsp70 levels in whole brain homogenates were analyzed by ELISA. The level of Hsp70 was determined to be significantly higher in the animals dosed with 30 mg/kg or higher compared to vehicle treatment alone. This indicates that at 30 mg/kg the amount of **40** that crossed into the brain was sufficient to robustly inhibit brain Hsp90. Hence, alcohol **40** appears to be a good tool compound to examine the effect of Hsp90 inhibition in the brain after a single acute dose. It should be noted, however, that a dose of 30 mg/kg is 3 times higher than what would be tolerated upon a repeated daily dosing, suggesting that neurological effects may not be detectable at therapeutically relevant doses and that **40** may

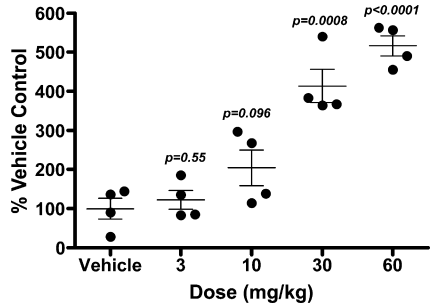

Figure 7. Pharmacodynamic effect of **40** on Hsp70 levels in the brain, following administration of a single oral dose in B6D2F1 female mice. HSP70 levels in brain homogenates were determined by ELISA and analyzed for statistical significance using unpaired two-tailed *t* test.

be ill-suited for neurological indications that would require repeated daily dosing.

10. CONCLUSION

In summary, the second-generation Hsp90 inhibitor **40** is an orally available compound that is substantially more potent than the first generation clinical inhibitor **14**. Compound **40** binds Hsp90α with K_i = 0.2 nM (vs 1.7 nM for the first-generation purine **14**). In MCF-7 cells, **40** induces Her-2 degradation with EC_{50} = 14 ± 5 nM and is 3 times more potent than **14** (EC_{50} = 38 ± 13 nM for **14**). In mouse, the plasma exposure upon a single oral dose of 25 mg/kg is 4419 ng·h/mL, while **14** is required to be dosed at 100 mg/kg to give a comparable exposure. Compound **40** is not a PGP substrate and is not actively effluxed by CACO-2 cells. In an N87 gastric tumor model, compound **40** completely blocks tumor growth at 5 mg/kg upon oral daily dosing (po, qd×5) and causes partial tumor regressions at 10 mg/kg. This is an improvement of over 20-fold with respect to **14**, which completely blocks tumor growth only at 120 mg/kg (po, qd×5) and does not induce regressions. Compound **40** is also active at 8 mg/kg in a NCI295 adrenocortical carcinoma that overexpresses PGP and against which the PGP substrate 17-AAG is inactive at 60 mg/kg.

We also investigated applications of **40** that would extend beyond the scope of oncology. We reported in a separate publication that **40** halts disease progression in rodent models of arthritis.[34] As for possible neurological indications, **40** is brain permeable (brain/plasma AUC ratio of 2.2), and a single oral dose of 30 mg/kg inhibits Hsp90 in the brains of mice, as witnessed by the up-regulation of brain Hsp70. The effect was statistically significant at 30 mg/kg but not at 10 mg/kg. Since the MTD for repeated daily dosing is 10 mg/kg, we conclude that **40** may not be well-suited to treat neurological indications. However, compound **40** remains of interest for severe inflammatory conditions and has a strong potential for the treatment of cancer.

■ ASSOCIATED CONTENT

Supporting Information

Preparation of iodide **27** and of Hsp90 inhibitors **35**−**41**. This material is available free of charge via the Internet at http://pubs.acs.org.

■ AUTHOR INFORMATION

Corresponding Author

*Phone: (858) 999-2360. E-mail: marco.biamonte@ddtd.org.

Notes

The authors declare no competing financial interest.

■ ACKNOWLEDGMENTS

The authors thank the following persons for their contribution to the in vitro and in vivo pharmacokinetic data: Reggie Angeles, Cheryl Black, Robin Caputo, Min Chang, Lawrence Gan, Julia Kaplan, Samina Khan, Eric Sands, Dong Wei, Chichih Wu, and Liyu Yang.

■ ABBREVIATIONS USED

17-AG, 17-amino-17-desmethoxygeldanamycin; 17-AAG, 17-allylamino-17-desmethoxygeldanamycin; AD, Alzheimer's disease; AUC, total area under the drug concentration−time curve; BSA, *N*,*O*-bis(trimethylsilyl)acetamide; C_{max}, maximum plasma drug concentration during a dosing interval; Cl, total clearance of drug in plasma; CMC, carboxymethylcellulose; 17-DMAG, 17-desmethoxy-17-*N*,*N*-dimethylaminoethylaminodesmethoxygeldanamycin; HR+ mBC, hormone receptor positive metastatic breast cancer; HSP, heat shock protein; MM, multiple myeloma; MTD, maximum tolerated dose; NIS, *N*-iodosuccinimide; NSCLC, non-small-cell lung cancer; PGP, P-glycoprotein; qd×5, daily dosing 5 days on (Monday−Friday) and 2 days off (Saturday−Sunday) (Latin: quaque die = daily); RECIST, response evaluation criteria in solid tumors; T_{max}, time after dosing when at maximum plasma drug concentration

■ REFERENCES

(1) (a) Neckers, L.; Workman, P. Hsp90 molecular chaperone inhibitors: are we there yet? *Clin. Cancer Res.* **2012**, *18*, 64−76. (b) Massey, A. J. ATPases as drug targets: insights from heat shock proteins 70 and 90. *J. Med. Chem.* **2010**, *53*, 7280−7286. (c) Biamonte, M. A.; Van De Water, R.; Perret, D.; Arndt, J. W.; Scannevin, R. H.; Lee, W.-C. Heat shock protein 90: Inhibitors in clinical trials. *J. Med. Chem.* **2010**, *53*, 3−17.

(2) HSP90 Interactors. http://www.picard.ch/downloads/Hsp90interactors.pdf.

(3) Schnur, R. C.; Corman, M. L.; Gallaschun, R. J.; Cooper, B. A.; Dee, M. F.; Doty, J. L.; Muzzi, M. L.; DiOrio, C. I.; Barbacci, E. G.; Miller, P. E.; Pollack, V. A.; Savage, D. M.; Sloan, D. E.; Pustilnik, L. R.; Moyer, J. D.; Moyer, M. P. erbB-2 oncogene inhibition by geldanamycin derivatives: synthesis, mechanism of action, and structure−activity relationships. *J. Med. Chem.* **1995**, *38*, 3813−3820.

(4) Ge, J.; Normant, E.; Porter, J. R.; Ali, J. A.; Dembski, M. S.; Gao, Y.; Georges, A. T.; Grenier, L.; Pak, R. H.; Patterson, J.; Sydor, J. R.; Tibbits, T. T.; Tong, J. K.; Adams, J.; Palombella, V. J. Design, synthesis, and biological evaluation of hydroquinone derivatives of 17-amino-17-demethoxygeldanamycin as potent, water-soluble inhibitors of HSP90. *J. Med. Chem.* **2006**, *49*, 4606−4615.

(5) (a) Glaze, E. R.; Smith, A. C.; Johnson, D. W.; McCormick, D. L.; Brown, A. B.; Levin, B. S.; Krishnaraj, R.; Lyubimov, A.; Egorin, M. J.; Tomaszewski, J. E. Dose range-finding toxicity studies of 17-DMAG. *Proc. Am. Assoc. Cancer Res.* **2003**, *44*, 162−162. (b) Eiseman, J. L.; Lan, J.; Lagatutta, T. F.; Hamburger, D. R.; Joseph, E.; Covey, J. M.; Egorin, M. J. Pharmacokinetics and pharmacodynamics of 17-demethoxy 17-[[(2-dimethylamino)ethyl]amino]geldanamycin (17DMAG, NSC 707545) in C.B-17 SCID mice bearing MDA-MB-231 human breast cancer xenografts. *Cancer Chemother. Pharmacol.* **2005**, *55*, 21−32.

(6) IPI-493, a Potent, Orally Bioavailable Hsp90 Inhibitor of the Ansamycin Class. http://infi.com/pipeline-archives/IPI-493%20EORTC%202008.pdf.

(7) Brough, P. A.; Aherne, W.; Barril, X.; Borgognoni, J.; Boxall, K.; Cansfield, J. E.; Cheung, K.-M. J.; Collins, I.; Davies, N. G. M.; Drysdale, M. J.; Dymock, B.; Eccles, S. A.; Finch, H.; Fink, A.; Hayes, A.; Howes, R.; Hubbard, R. E.; James, K.; Jordan, A. M.; Lockie, A.; Martins, V.; Massey, A.; Matthews, T. P.; McDonald, E.; Northfield, C. J.; Pearl, L. H.; Prodromou, C.; Ray, S.; Raynaud, F. I.; Roughley, S. D.; Sharp, S. Y.; Surgenor, A.; Walmsley, D. L.; Webb, P.; Wood, M.; Workman, P.; Wright, L. 4,5-Diarylisoxazole HSP90 chaperone inhibitors: potential therapeutic agents for the treatment of cancer. *J. Med. Chem.* **2008**, *51*, 196−218.

(8) Woodhead, A. J; Angove, H.; Carr, M. G.; Chessari, G.; Congreve, M.; Coyle, J. E.; Cosme, J.; Graham, B.; Day, P. J.; Downham, R.; Fazal, L.; Feltell, R.; Figueroa, E.; Frederickson, M.; Lewis, J.; McMenamin, R.; Murray, C. W.; O'Brien, M. A.; Parra, L.; Patel, S.; Phillips, T.; Rees, D. C.; Rich, S.; Smith, D.-M.; Trewartha, G.; Vimkovic, M.; Williams, B.; Woolford, A. J. Discovery of (2,4-dihydroxy-5-isopropylphenyl)-[5-(4-methylpiperazin-1-yl-methyl)-1,3-dihydroisondol-2-yl]methanone (AT13387), a novel inhibitor of the molecular chaperone Hsp90 by fragment based drug design. *J. Med. Chem.* **2010**, *53*, 5956−5969.

(9) Ying, W.; Du, Z.; Sun, L.; Foley, K. P.; Proia, D. A.; Blackman, R. K.; Zhou, D.; Inoue, T.; Tatsuta, N.; Sang, J.; Ye, S.; Acquaviva, J.; Ogawa, L. S.; Wada, Y.; Barsoum, J.; Koya, K. Ganetespib, a unique triazolone-containing Hsp90 inhibitor, exhibits potent antitumor activity and a superior safety profile for cancer therapy. *Mol. Cancer Ther.* **2012**, *11*, 475−484.

(10) Nakashima, T.; Ishii, T.; Tagaya, H.; Seike, T.; Nakagawa, H.; Kanda, Y.; Akinaga, S.; Soga, S.; Shiotsu, Y. New molecular and biological mechanism of antitumor activities of KW-2478, a novel nonansamycin heat shock protein 90 inhibitor, in multiple myeloma cells. *Clin. Cancer Res.* **2010**, *16*, 2792−2802.

(11) (a) Immormino, R. M; Kang, Y.; Chiosis, G.; Gewirth, D. T. Structural and quantum chemical studies of 8-aryl-sulfanyl adenine class Hsp90 inhibitors. *J. Med. Chem.* **2006**, *49*, 4953−4960. (b) Caldas-Lopes, E.; Cerchietti, L.; Ahn, J. H.; Clement, C. C.; Robles, A. I.; Rodina, A.; Moulick, K.; Taldone, T.; Gozman, A.; Guo, Y.; Wu, N.; de Stanchina, E.; White, J.; Gross, S. S.; Ma, Y.; Varticovski, L.; Melnick, A.; Chiosis, G. Hsp90 inhibitor PU-H71, a multimodal inhibitor of malignancy, induces complete responses in triple-negative breast cancer models. *Proc. Natl. Acad. Sci. U.S.A.* **2009**, *106*, 8368−8373.

(12) Bao, R.; Lai, C.-J.; Qu, H.; Wang, D.; Yin, L.; Zifcak, B.; Atoyan, R.; Wang, J.; Samson, M.; Forrester, J.; Della Rocca, S.; Xu, G.-X.; Tao, X.; Zhai, H.-X.; Cai, X.; Qian, C. CUDC-305, a novel synthetic HSP90 inhibitor with unique pharmacologic properties for cancer therapy. *Clin. Cancer Res.* **2009**, *15*, 4046−4057.

(13) Evaluation of the Pharmacokinetics and Efficacy of a Novel Pro-Drug of the HSP90 Inhibitor. http://www.myriadpharma.com/images/stories/product-pipeline/mpc-3100/AACR%202011/aacr-2011-abst3237-mpc-3100-prodrug-mpc-0767.pdf.

(14) Fadden, P.; Huang, K. H.; Veal, J. M.; Steed, P. M.; Barabasz, A. F.; Foley, B.; Hu, M.; Partridge, J. M.; Rice, J.; Scott, A.; Dubois, L. G.; Freed, T. A.; Silinski, M. A.; Barta, T. E.; Hughes, P. F.; Ommen, A.; Ma, W.; Smith, E. D.; Spangenberg, A. W.; Eaves, J.; Hanson, G. J.; Hinkley, L.; Jenks, M.; Lewis, M.; Otto, J.; Pronk, G. J.; Verleysen, K.; Haystead, T. A.; Hall, S. E. Application of chemoproteomics to drug discovery: identification of a clinical candidate targeting hsp90. *Chem. Biol.* **2010**, *17*, 686−694.

(15) Kasibhatla, S. R.; Hong, K.; Biamonte, M. A.; Busch, D. J.; Karjian, P. L.; Sensintaffar, J. L.; Kamal, A.; Lough, R. E.; Brekken, J.; Lundgren, K.; Grecko, R.; Timony, G. A.; Ran, Y.; Mansfield, R.; Fritz, L. C.; Ulm, E.; Burrows, F. J.; Boehm, M. F. Rationally designed high-affinity 2-amino-6-halopurine heat shock protein 90 inhibitors that exhibit potent antitumor activity. *J. Med. Chem.* **2007**, *50*, 2767−2778.

(16) (a) Menezes, D. L.; Taverna, P.; Jensen, M. R.; Abrams, T.; Stuart, D.; Yu, G. K.; Duhl, D.; Machajewski, T.; Sellers, W. R.; Pryer, N. K.; Gao, Z. The novel oral Hsp90 inhibitor NVP-HSP990 exhibits potent and broad-spectrum antitumor activities in vitro and in vivo. *Mol. Cancer Ther.* **2012**, *11*, 730−739. (b) For another series, also from Novartis, see the following: Massey, A. J.; Schoepfer, J.; Brough, P. A.; Brueggen, J.; Chene, P.; Drysdale, M. J.; Pfaar, U.; Radimerski, T.; Ruetz, S.; Schweitzer, A.; Wood, M.; Garcia-Echeverria, C.; Jensen, M. R. Preclinical antitumor activity of the orally available heat shock

protein 90 inhibitor NVP-BEP800. *Mol. Cancer Ther.* **2010**, *9*, 906−919.
(17) Modi, S.; Stopeck, A.; Linden, A.; Solit, D.; Chandarlapaty, S.; Rosen, N.; D'Andrea, G.; Dickler, M.; Moynahan, M. E.; Sugarman, S.; Ma, W.; Patil, S.; Norton, L.; Hannan, A. L.; Hudis, C. Hsp90 inhibition is effective in breast cancer: a phase II trial of tanespimycin (17-AAG) plus trastuzumab in patients with Her-2 positive metastatic breast cancer progressing on trastuzumab. *Clin. Cancer Res.* **2011**, *17*, 5132−5139.
(18) Wong, K. K.; Koczywas, M.; Goldman, J. W.; Paschold, E. H.; Horn, L.; Lufkin, J. M.;Kepros, J.; Teofilici, F.; Shapiro, G.; Socinski, M. A. An Open-Label Phase II Study of the Hsp90 Inhibitor Ganetespib. (STA-9090) as Monotherapy in Patients with Advanced NSCLC. Presented at the ASCO Annual Meeting, 2011; http://www.syntapharma.com/Documents/Ganetespib_Phase%202%20NSCLC_Shapiro_ASCO%202011.pdf.
(19) Sequist, L. V.; Gettinger, S.; Senzer, N. N.; Martins, R. G.; Jänne, P. A.; Lilenbaum, R.; Gray, J. E.; Iafrate, A. J.; Katayama, R.; Hafeez, N.; Sweeney, J.; Walker, J. R.; Fritz, C.; Ross, R. W.; Grayzel, D.; Engelman, J. A.; Borger, D. R.; Paez, G.; Natale, R. Activity of IPI-504, a novel heat-shock protein 90 inhibitor, in patients with molecularly defined non-small-cell lung cancer. *J. Clin. Oncol.* **2010**, *28*, 4953−4960.
(20) Katayama, R.; Khan, T. M.; Benes, C.; Lifshits, E.; Ebi, H.; Rivera, V. M.; Shakespeare, W. C.; Iafrate, A. J.; Engelman, J. A.; Shaw, A. T. Therapeutic strategies to overcome crizotinib resistance in non-small cell lung cancers harboring the fusion oncogene EML4-ALK. *Proc. Natl. Acad. Sci. U.S.A.* **2011**, *108*, 7535−7540.
(21) (a) Richardson, P G.; Chanan-Khan, A. A.; Lonial, S.; Krishnan, A. Y.; Carroll, M. P.; Alsina, M.; Albitar, M.; Berman, D.; Messina, M.; Anderson, K. C. Tanespimycin and bortezomib combination treatment in patients with relapsed or relapsed and refractory multiple myeloma: results of a phase 1/2 study. *Br. J. Haematol.* **2011**, *153*, 729−740. (b) Richardson, P. G.; Mitsiades, C. S.; Laubach, J. P.; Lonial, S.; Chanan-Khan, A. A; Anderson, K. C. Inhibition of heat shock protein 90 (HSP90) as a therapeutic strategy for the treatment of myeloma and other cancers. *Br. J. Haematol.* **2011**, *152*, 367−379.
(22) Yin, Z.; Zhang, H.; Lundgren, K.; Wilson, L.; Burrows, F.; Shores, C. G. BIIB021, a novel Hsp90 inhibitor, sensitized head and neck squamous cell carcinoma to radiotherapy. *Int. J. Cancer* **2010**, *126*, 1216−1225.
(23) Infante, J.; Weiss, G.; Jones, S.; Tibes, R.; Bendell, J.; Brega, N.; Torti, V.; Von Hoff, D.; Burris, H., III; Ramanathan, R. Phase 1 dose escalation study of the oral heat shock protein 90 (Hsp90) inhibitor PF-04929113/SNX-5422 (PF-113) and its associated ocular toxicity. *EJC Suppl.* **2010**, *8*, 119.
(24) (a) Huang, K. H.; Eaves, J.; Veal, J.; Barta, T.; Lifeng, G.; Hinkley, L.; Hanson, G. Tetrahydroindolone and Tetrahydroindazolone Derivatives, WO 2006/091963, 2006. (b) Huang, K. H.; Eaves, J.; Veal, J.; Hall, S. E.; Barta, T. E.; Hanson, G. J. Cyclohexylamino Benzene, Pyridine, and Pyridazine Derivatives. US 2007/0207984, 2007.
(25) Lundgren, K.; Zhang, H.; Brekken, J.; Huser, N.; Powell, R. E.; Timple, N.; Busch, D. J.; Neely, L.; Sensintaffar, J. L.; Yang, Y.-C.; McKenzie, A.; Friedman, J.; Scannevin, R.; Kamal, A.; Hong, K.; Kasibhatla, S. R.; Boehm, M. F.; Burrows, F. J. BIIB021, an orally available, fully synthetic small molecule inhibitor of the heat shock protein HSP90. *Mol. Cancer Ther.* **2009**, *8*, 921−929.
(26) Miller, D. J.; Ravikumar, K.; Shen, H.; Suh, J.-K.; Kerwin, S. M.; Robertus, J. D. Structure-based and characterization of novel platforms for ricin and shiga toxin inhibition. *J. Med. Chem.* **2002**, *45*, 90−98.
(27) Taylor, E. C.; Kuhnt, D.; Shih, C.; Rinzel, S. M.; Grindey, G. B.; Barredo, J.; Jannatipour, M.; Moran, R. G. A dideazatetrahydrofolate analog lacking a chiral center at C-6: *N*-[4-[2-(2-amino-3,4-dihydro-4-oxo-7*H*-pyrrolo[2,3-*d*]pyrimidin-5yl)ethyl[benzoyl]-L-glutamic acid is an inhibitor of thymidylate synthase. *J. Med. Chem.* **1992**, *35*, 4450−4454.
(28) Gangjee, A.; Yu, J.; Kisliuk, R. L.; Haile, W. H.; Sobrero, G.; McGuire, J. J. Design, synthesis, and biological activities of classical *N*-{4-[2-(2-amino-4-ethylpyrrolo[2,3-*d*]pyrimidin-5-yl)ethyl]benzoyl}-L-glutamic acid and its 6-methyl derivative as potential dual inhibitors of thymidylate synthase and dihydrofolate reductase as potential antitumor agents. *J. Med. Chem.* **2003**, *46*, 591−600.
(29) Shih, C.; Gossett, L. S. The synthesis of *N*-{2-amino-4-substituted [(pyrrolo[2,3-*d*]pyrimidin-5-yl)ethyl]benzoyl}-L-glutamic acids as antineoplastic agents. *Heterocycles* **1993**, *35*, 825−841.
(30) Seela, F.; Peng, X. Regioselective syntheses of 7-halogenated 7-deazapurine nucleosides related to 2-amino-7-deaza-2′-deoxyadenosine and 7-deaza-2′-deoxyisoguanosine. *Synthesis* **2004**, 1203−1210.
(31) Barnett, C. J.; Kobierski, M. E. A convenient method for regioselective C-5 halogenation of 4(3*H*)-oxo-7*H*-pyrrolo[2,3-*d*]-pyrimidines. *J. Heterocycl. Chem.* **1994**, *31*, 1181−1183.
(32) Tu, Y. Q.; Huebener, A.; Zhang, H.; Moore, C. J.; Fletcher, M. T.; Hayes, P.; Dettner, K.; Francke, W.; McErlean, C. S. P.; Kitching, W. Synthesis and stereochemistry of insect derived spiroacetals with branched carbon skeletons. *Synthesis* **2000**, *13*, 1956−1978.
(33) The sterically bulky *gem*-dimethyl group of **40** was designed to maximize the metabolic stability of **40** by simultaneously hindering any potential phase I metabolism at the adjacent propargylic position and any potential phase II metabolism of the OH group. This may be a reason for the improved pharmacokinetic properties.
(34) Yun, T. J.; Harning, E. K.; Giza, K.; Rabah, D.; Li, P.; Arndt, J. W.; Luchetti, D.; Biamonte, M. A.; Shi, J.; Lundgren, K.; Manning, A.; Kehry, M. R. EC144, a synthetic inhibitor of heat shock protein 90, blocks innate and adaptive immune responses in models of inflammation and autoimmunity. *J. Immunol.* **2011**, *186*, 563−575.
(35) Compounds **14** and **40** were dosed in 0.1 N HCl for the xenograft models.
(36) (a) Huang, Y.; Blower, P. E.; Liu, R.; Dai, Z.; Pham, A. N.; Moon, H.; Fang, J.; Sadée, W. Chemogenomic analysis indentifies geldanamycins as substrated and inhibitors of ABCB1. *Pharm. Res.* **2007**, *9*, 1702−1712. (b) Zhang, H.; Neely, L.; Yang, Y.-C.; Timple, N.; Burrows, F. BIIB021, a synthetic Hsp90 inhibitor, has broad application against tumors with acquired multidrug resistance. *Int. J. Cancer* **2009**, *126*, 1226−1234.
(37) Luo, W.; Rodina, A.; Chiosis, G. Heat shock protein 90: translation from cancer to Alzheimer's disease treatment? *BMC Neurosci.* **2008**, *9* (Suppl. 2), S7.
(38) Luo, W.; Dou, F.; Rodina, A.; Chip, S.; Kim, J.; Zhao, Q.; Moulick, K.; Aguirre, J.; Wu, N.; Greengard, P.; Chiosis, G. Roles of heat-shock protein 90 in maintaining and facilitating the neurodegenerative phenotype in tauopathies. *Proc. Natl. Acad. Sci. U.S.A.* **2007**, *104*, 9511−9516.
(39) Dickey, C. A.; Dunmore, J.; Lu, B.; Wang, J.-W.; Lee, W. C.; Kamal, A.; Burrows, F.; Eckman, C.; Hutton, M.; Petrucelli, L. HSP induction mediates selective clearance of tau phosphorylated at proline-directed Ser/Thr sites but not KXGS (MARK) sites. *FASEB J.* **2006**, *20*, 753−755.
(40) Dickey, C. A.; Eriksen, J.; Kamal, A.; Burrows, F.; Kasibhatla, S.; Eckman, C. B.; Hutton, M.; Petrucelli, L. Development of a high throughput drug screening assay for the detection of changes in tau levels—proof of concept with HSP90 inhibitors. *Curr. Alzheimer Res.* **2005**, *2*, 231−238.
(41) Salminen, A.; Ojala, J.; Kaarniranta, K.; Hiltunen, M.; Soininen, H. Hsp90 regulates tau pathology through co-chaperone complexes in Alzheimer's disease. *Prog. Neurobiol.* **2011**, *93*, 99−110.